

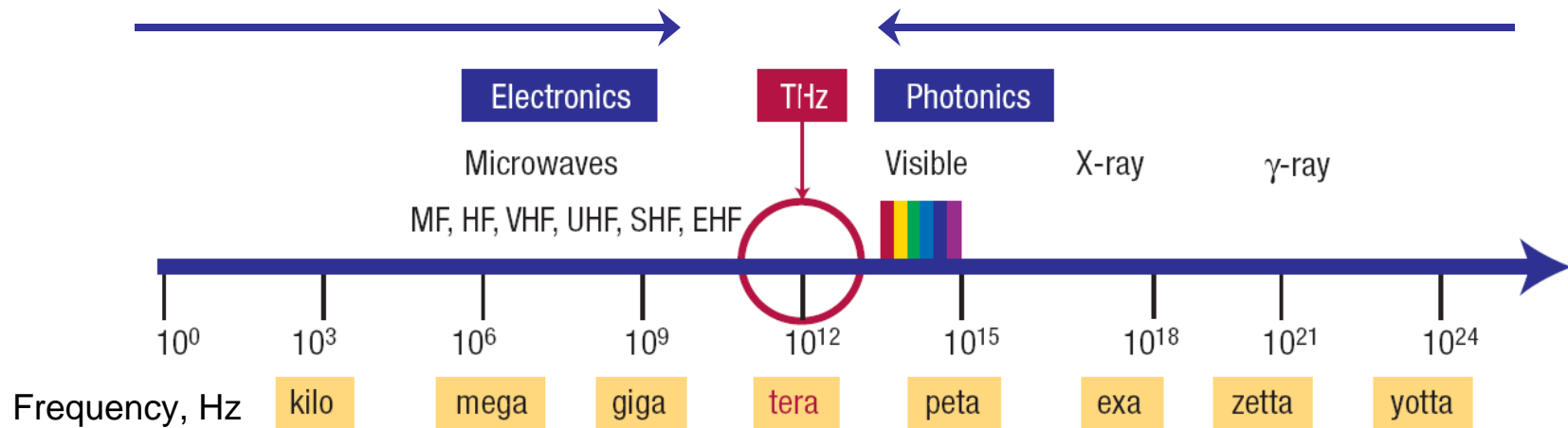
THz QCL sources for operation above cryogenic temperatures

Mikhail Belkin

*Department of Electrical and Computer Engineering
University of Texas at Austin*

IQCLSW, Monte Verita, Switzerland 2008

Need for semiconductor THz source

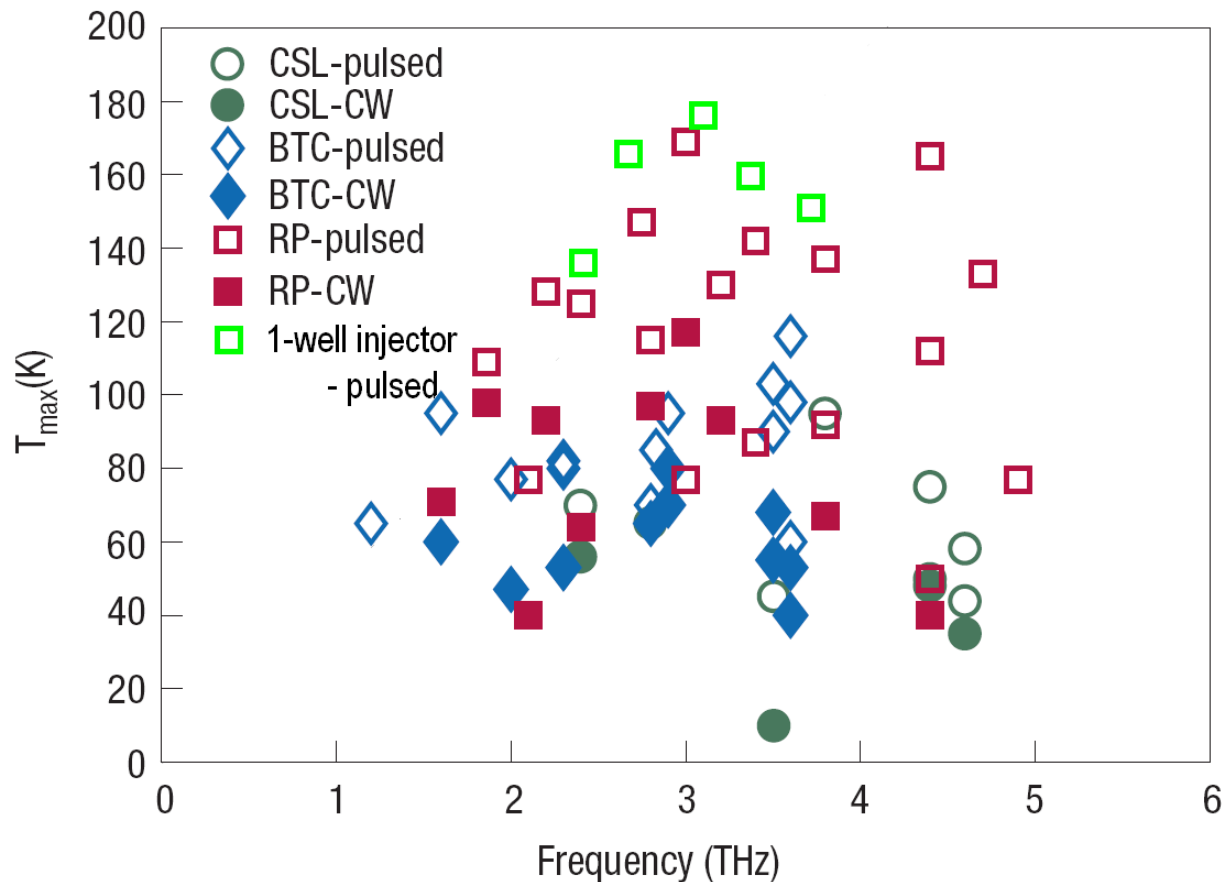


- Spectroscopy
- Local oscillator for THz heterodyning
- Remote sensing, screening, inspection, etc.
- THz frequency amplification

THz Quantum Cascade Lasers



Maximum operating temperature VS frequency



***BS Williams, Nature Photonics 1, 517-525 (2007) +
2008 data of Capasso, Colombelli, and Linfield groups***

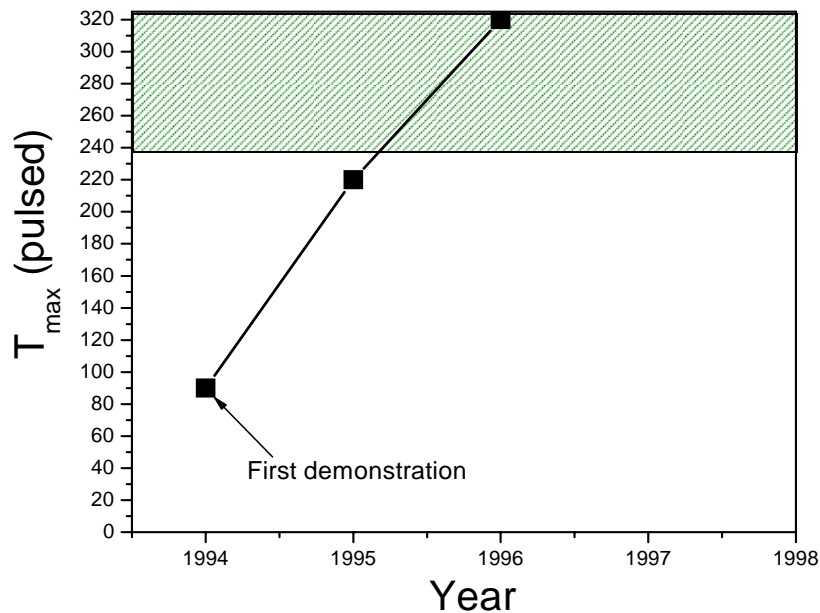
RT THz QCLs: very difficult



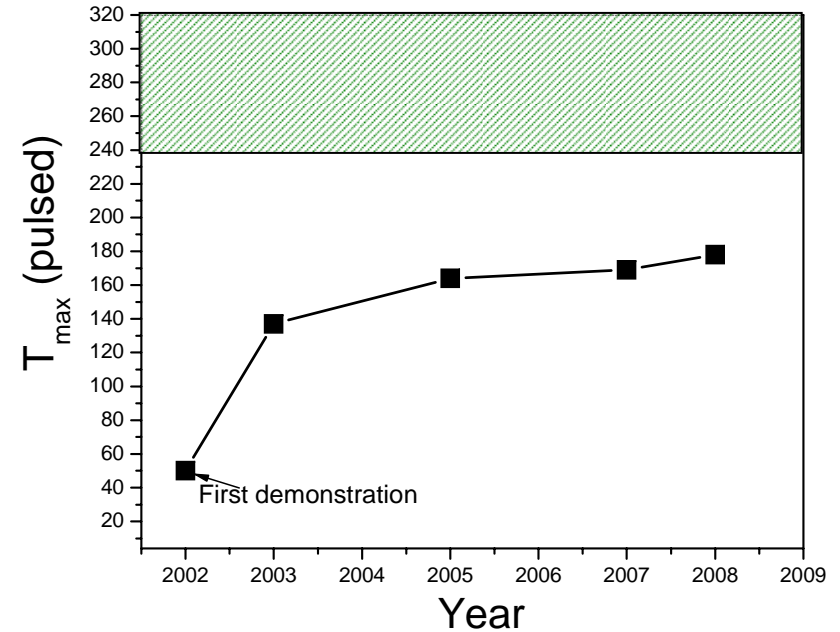
Upper state lifetime $< 2\text{ps}$ for temperature $> 200\text{K}$
This lifetime is similar to that in mid-IR QCLs

BUT, THz QCLs have higher w/g losses and smaller injection efficiency

Mid-IR QCLs



THz QCLs



Nevertheless, no fundamental limit on RT operation

Room-temperature THz source?



- 1. Investigate alternative designs, improve GaAs/AlGaAs quality, try different materials (InGaAs/AlInAs, Si/SiGe, AlGaN/GaN), low-dimensional systems (quantum dots, wires), etc.**
- 2. Develop semiconductor THz sources that do not require population inversion across the THz transition**

Room-temperature THz source?



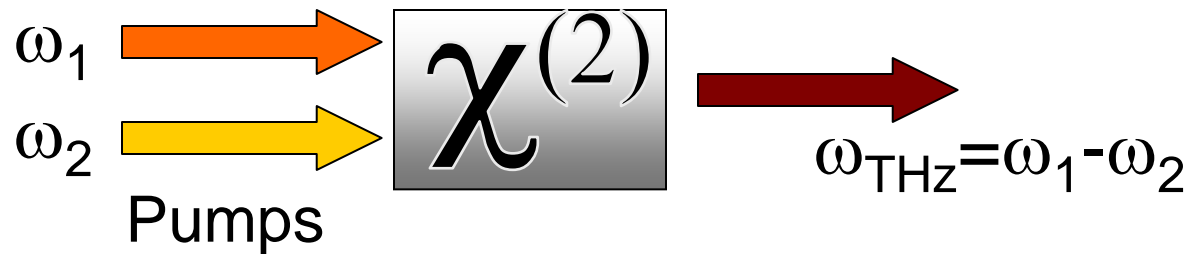
1. Investigate alternative designs, improve GaAs/AlGaAs quality, try different materials (InGaAs/AlInAs, Si/SiGe, AlGaN/GaN), low-dimensional systems (quantum dots, wires), etc.

2. Develop semiconductor THz sources that do not require population inversion across the THz transition

Difference Frequency Generation

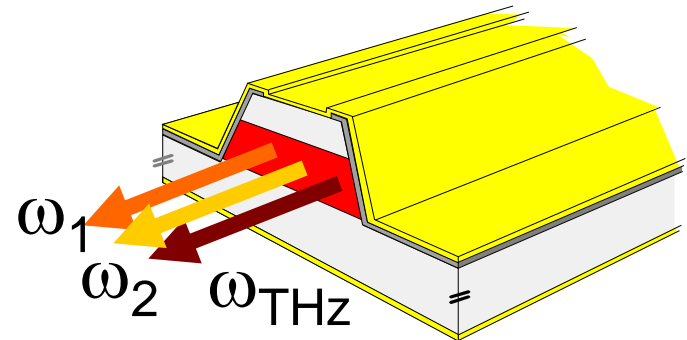


Difference-frequency generation (DFG) occurs in a medium with second-order nonlinear susceptibility $\chi^{(2)}$



THz QCL source using intra-cavity DFG

- *Dual-frequency mid-infrared QCLs with $\chi^{(2)}$*
- *THz radiation is generated via intra-cavity DFG*
- *Widely tunable THz source at RT*



Challenges for intra-cavity THz DFG



$$I(\omega_{THz}) \propto |\chi^{(2)}|^2 I(\omega_1) I(\omega_2) \times l_{coh}^2$$

$$l_{coh}^2 = \frac{1}{((k_1 - k_2 - k_{THz})^2 + (\alpha_{THz})^2)}$$

Solid-state systems

QCLs

$I(\omega_1), I(\omega_2)$

100 -1000 MW/cm²

1-10 MW/cm²

l_{coh}

$\gtrsim 10$ mm

$\lesssim 0.2$ mm

$\chi^{(2)}$

~ 100 pm/V

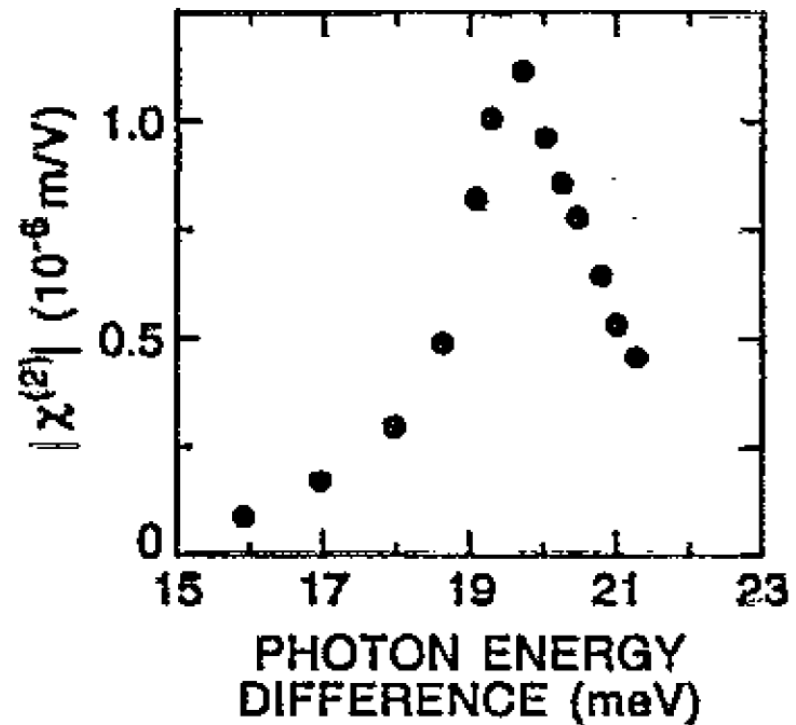
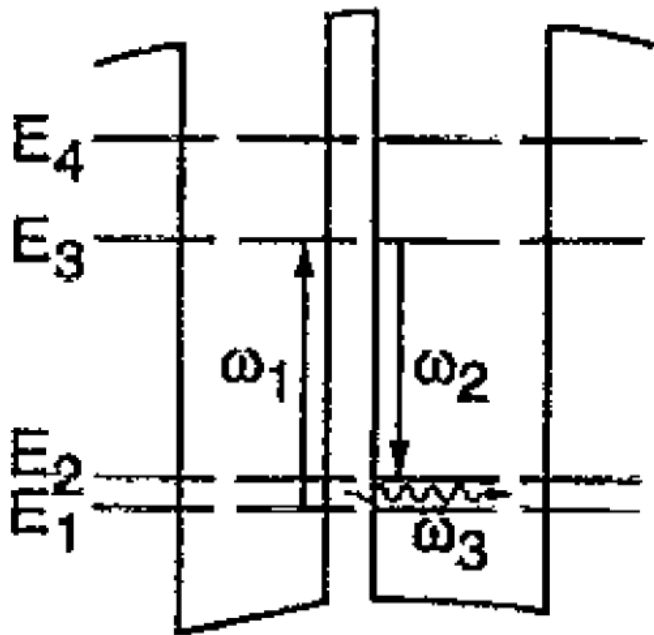
can be designed

Need giant $\chi^{(2)}$

Giant $\chi^{(2)}$ in quantum wells

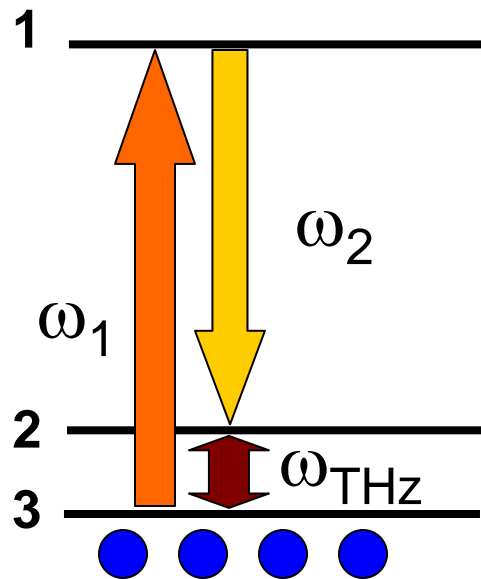


$$\chi^{(2)} = N_e \frac{e^3}{\hbar^2 \epsilon_0} \times \sum_{n,n'} \frac{z_{1n} z_{nn'} z_{n'1}}{(\omega - \omega_{nn'} + i\Gamma_{nn'})} \left(\frac{1}{(\omega_1 + \omega_{n'1} + i\Gamma_{n'1})} + \frac{1}{(-\omega_2 - \omega_{n1} + i\Gamma_{n1})} \right)$$



Sirtori et al., APL (1994)

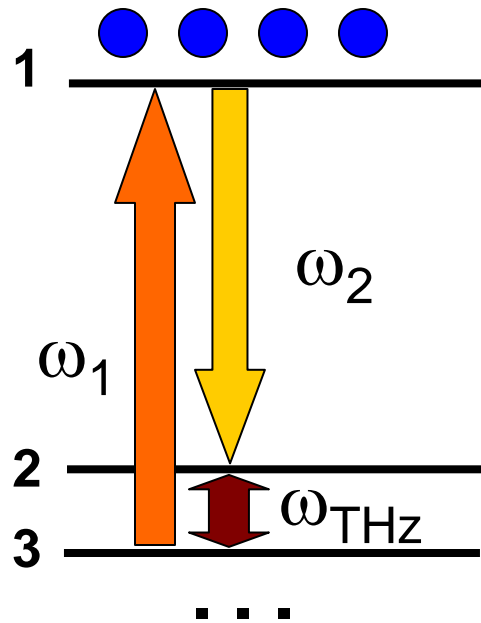
Giant $\chi^{(2)}$ in quantum wells



$$\chi^{(2)} = N_e \frac{e^3}{\hbar^2 \epsilon_0} \times \sum_{n,n'} \frac{z_{1n} z_{nn'} z_{n'1}}{(\omega - \omega_{nn'} + i\Gamma_{nn'})} \left(\frac{1}{(\omega_1 + \omega_{n'1} + i\Gamma_{n'1})} + \frac{1}{(-\omega_2 - \omega_{n1} + i\Gamma_{n1})} \right)$$

Giant absorption!

$\chi^{(2)}$ with population inversion

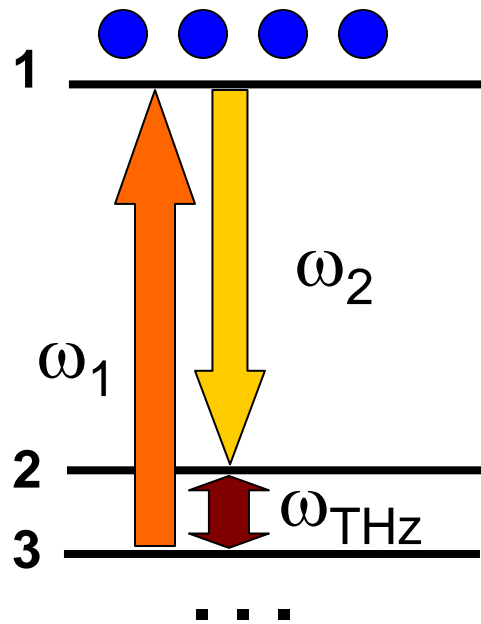


$$\chi^{(2)} = N_e \frac{e^3}{\hbar^2 \epsilon_0} \times \sum_{n,n'} \frac{z_{1n} z_{nn'} z_{n'1}}{(\omega - \omega_{nn'} + i\Gamma_{nn'})} \left(\frac{1}{(\omega_1 + \omega_{n'1} + i\Gamma_{n'1})} + \frac{1}{(-\omega_2 - \omega_{n1} + i\Gamma_{n1})} \right)$$

Laser action instead of absorption!

Gmachl, Belyanin, et al., JQE (2003)

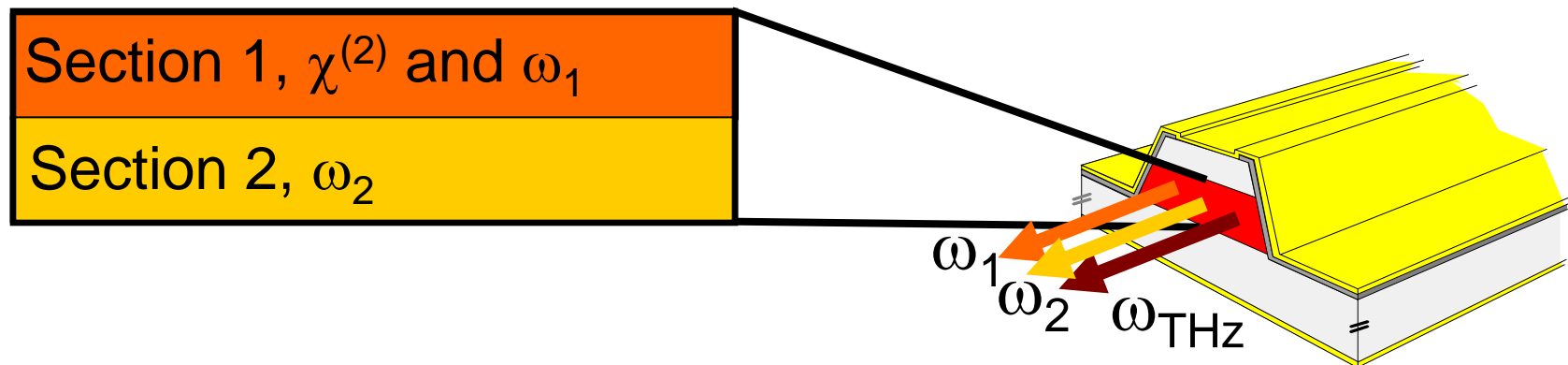
$\chi^{(2)}$ with population inversion



$$\chi^{(2)} = N_e \frac{e^3}{\hbar^2 \epsilon_0} \times \sum_{n,n'} \frac{z_{1n} z_{nn'} z_{n'1}}{(\omega - \omega_{nn'} + i\Gamma_{nn'})} \left(\frac{1}{(\omega_1 + \omega_{n1} + i\Gamma_{n1})} + \frac{1}{(-\omega_2 - \omega_{n1} + i\Gamma_{n1})} \right)$$

Laser action instead of absorption!

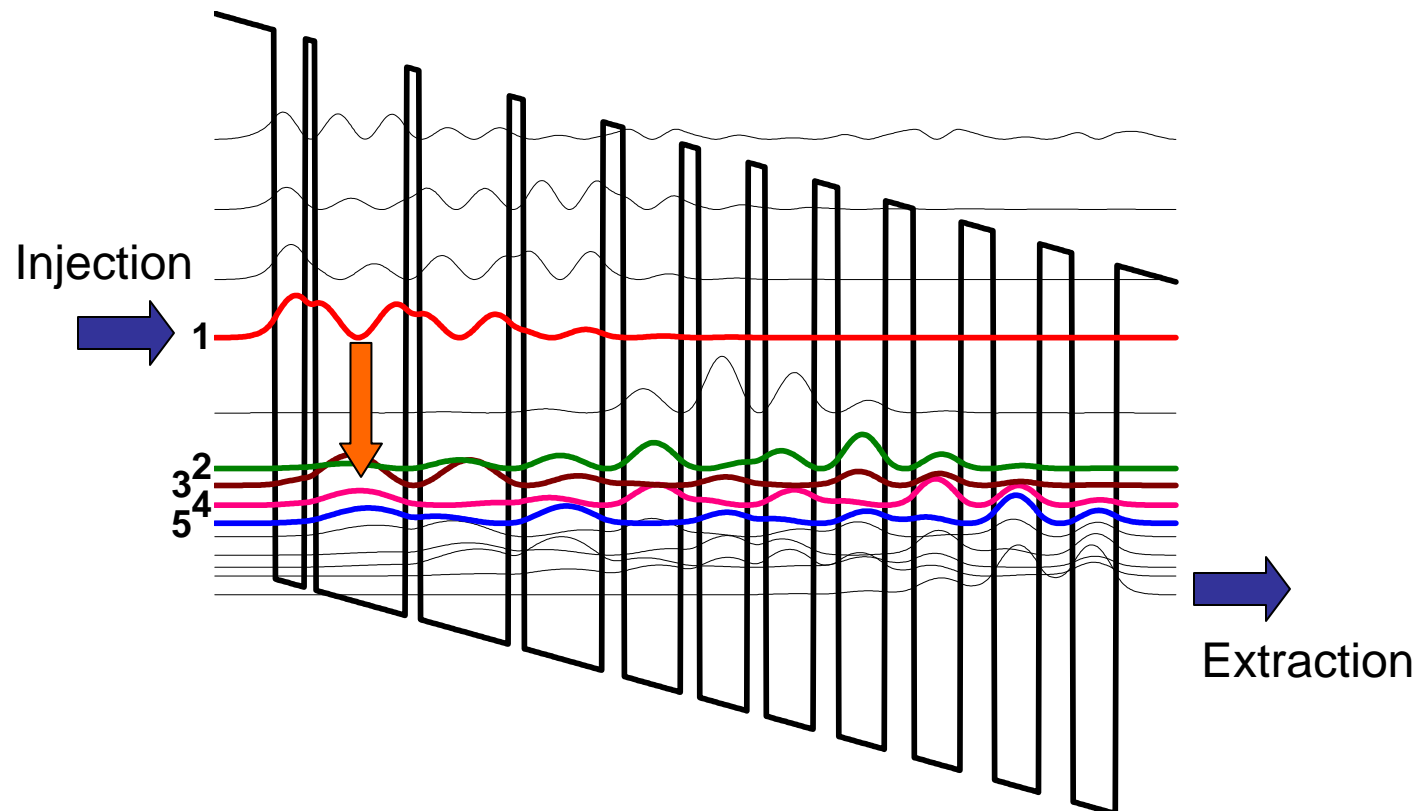
Active region design



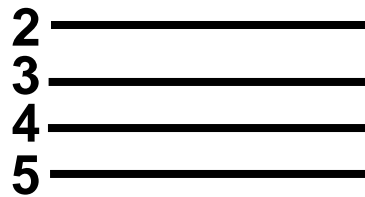
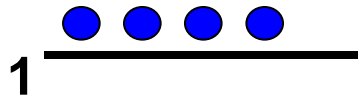
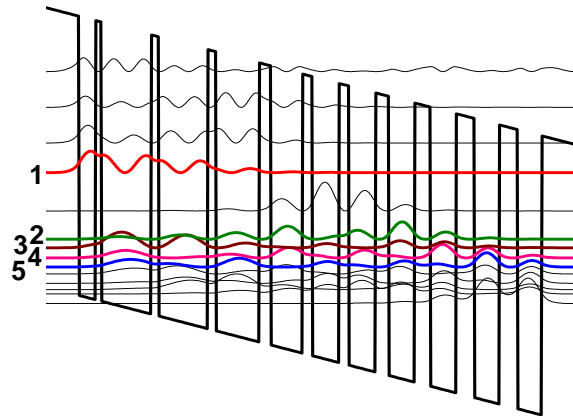
$\chi^{(2)}$ -section design

Bound-to-continuum active
region for $\lambda \approx 9\mu\text{m}$

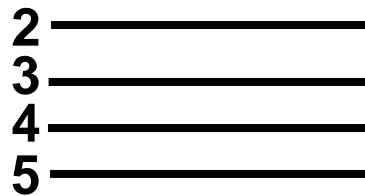
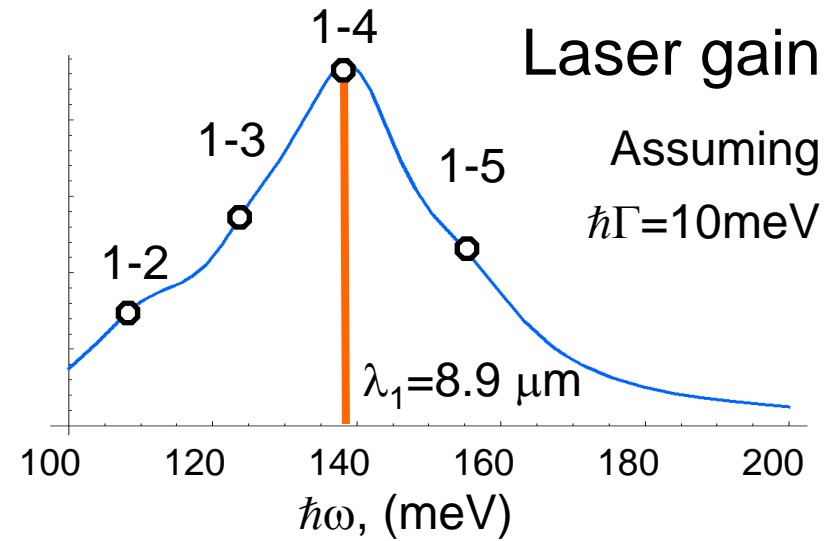
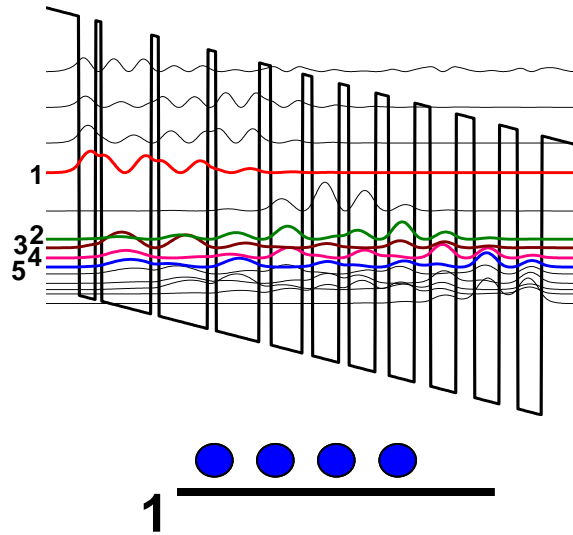
[Faist et al. IEEE JQE (2002)]



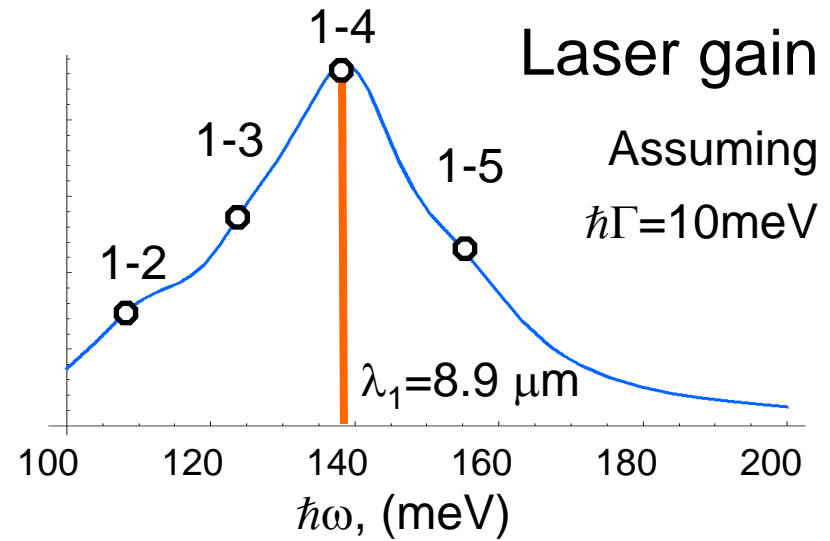
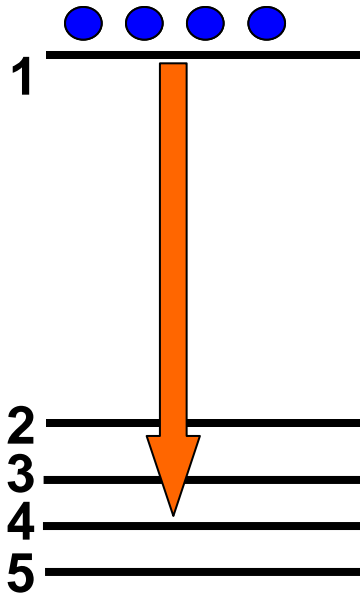
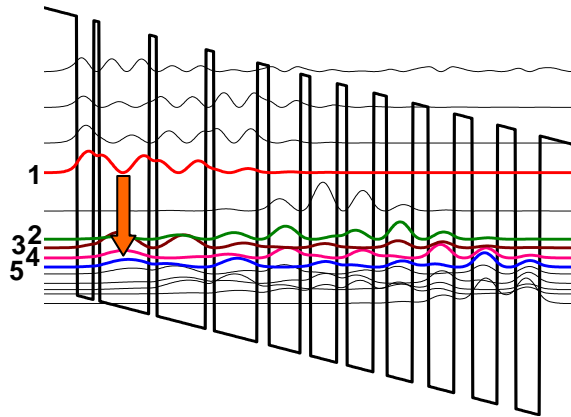
$\chi^{(2)}$ -section design



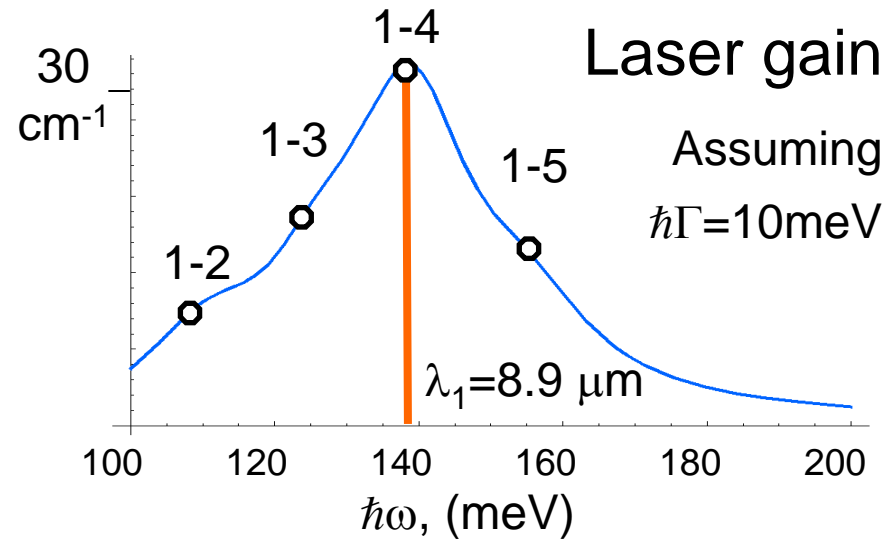
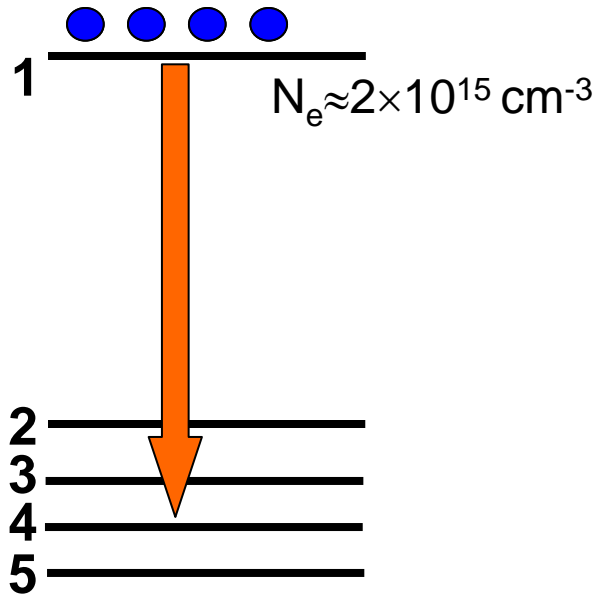
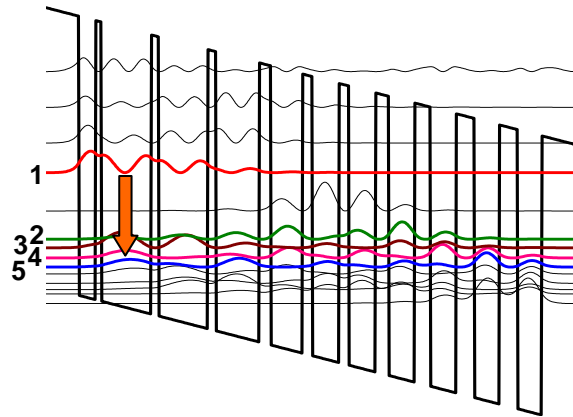
$\chi^{(2)}$ -section design



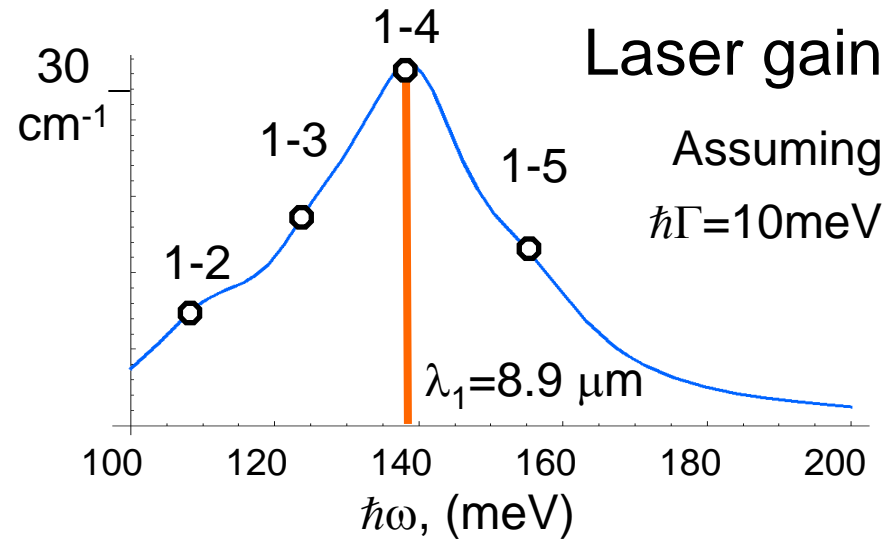
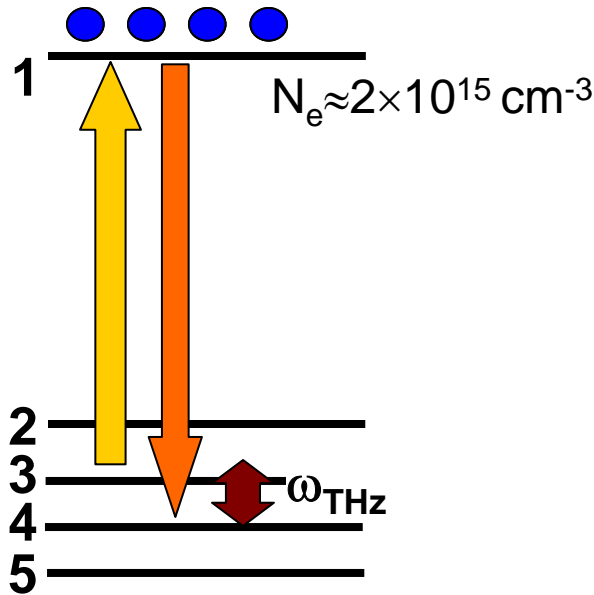
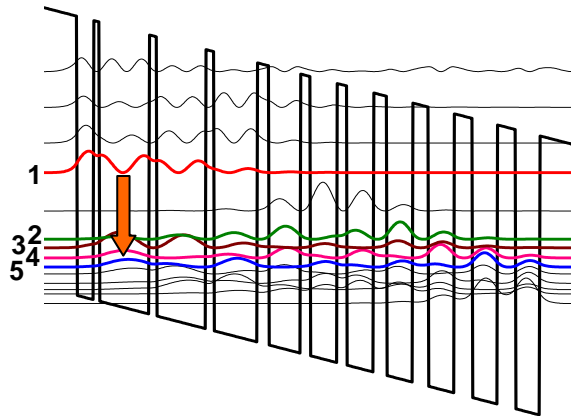
$\chi^{(2)}$ -section design



$\chi^{(2)}$ -section design



$\chi^{(2)}$ -section design

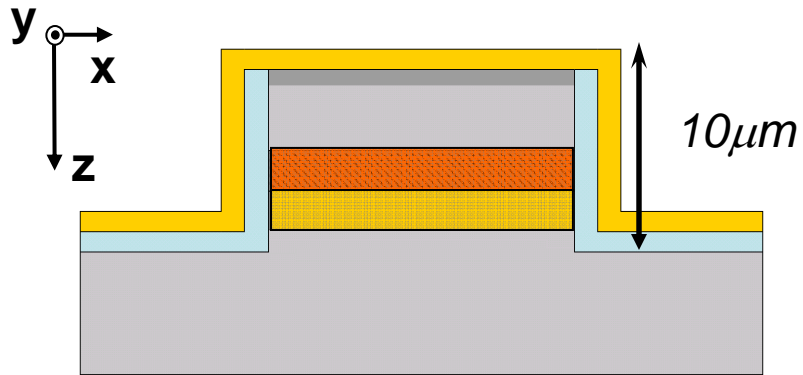


$$\lambda_1 = 8.9 \mu\text{m} \quad \Rightarrow \quad \lambda_{\text{THz}} = 60 \mu\text{m}$$

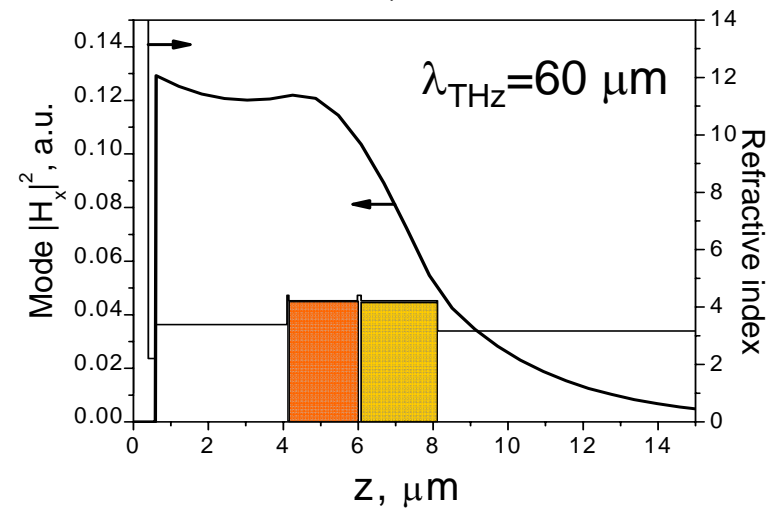
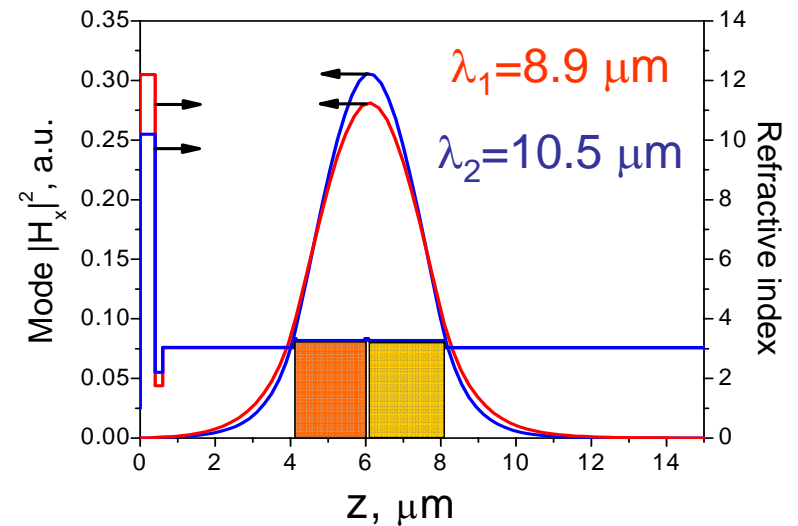
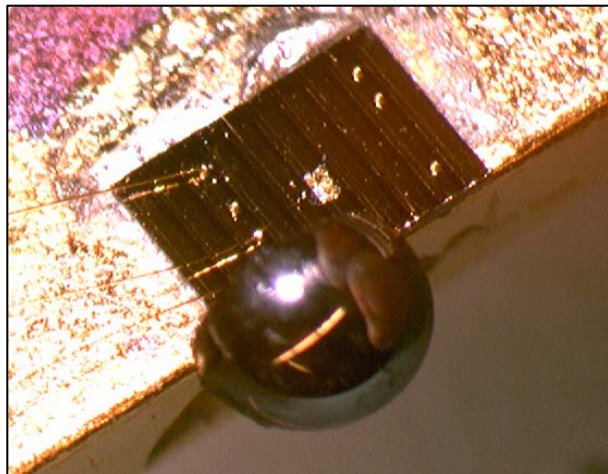
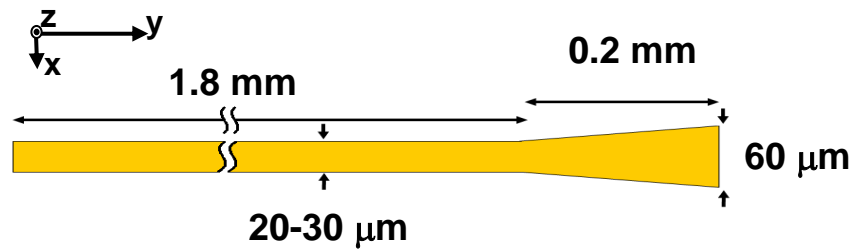
$$\lambda_2 = 10.5 \mu\text{m}$$

$$\chi^{(2)} \approx 3 \times 10^4 \text{ pm/V}$$

Waveguide design



30 stages of each QCL structure

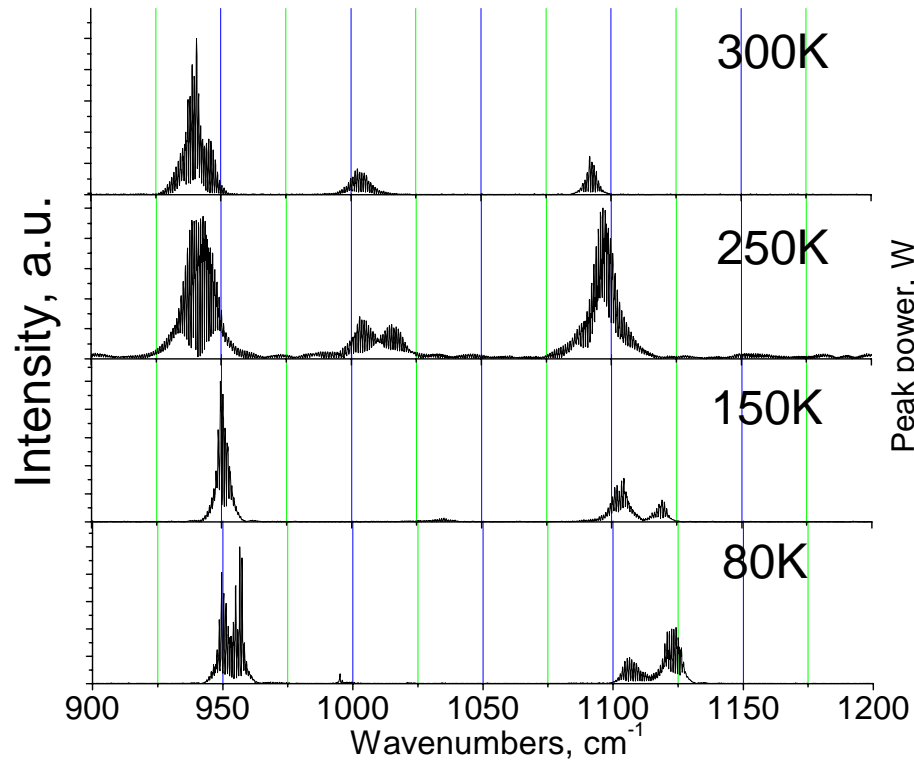


$$l_{coh} = 70 \mu m$$

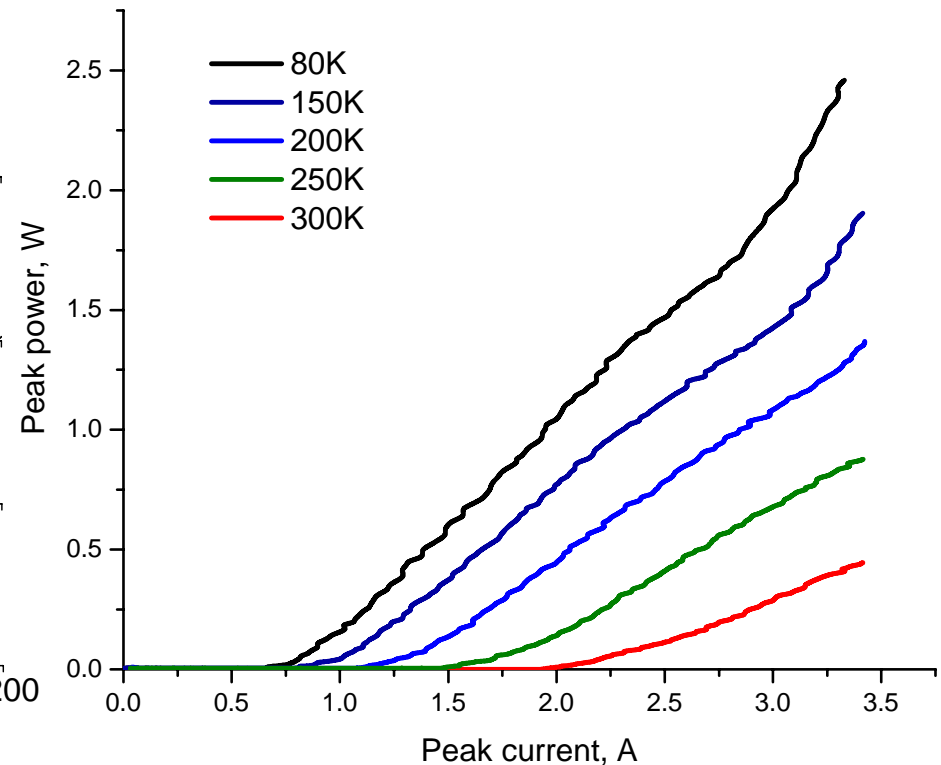
Device performance: mid-IR



Spectra



Power (combined)

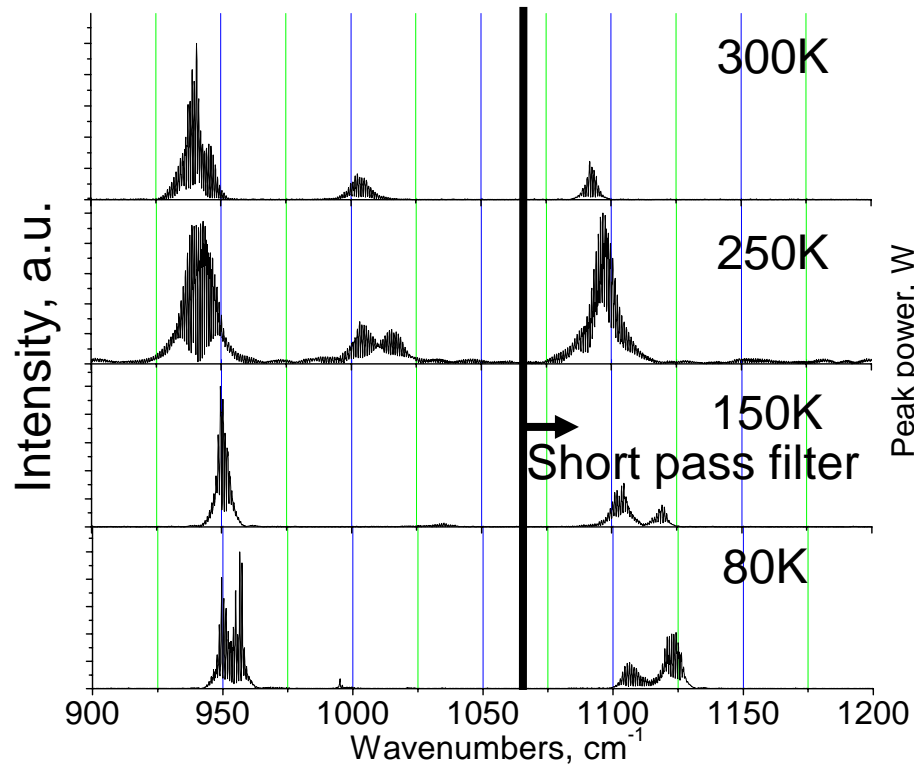


25- μm -wide, tapered to 50- μm -wide, 2-mm-long, back facet HR coating.
Testing in pulsed mode (60ns pulses at 250kHz).

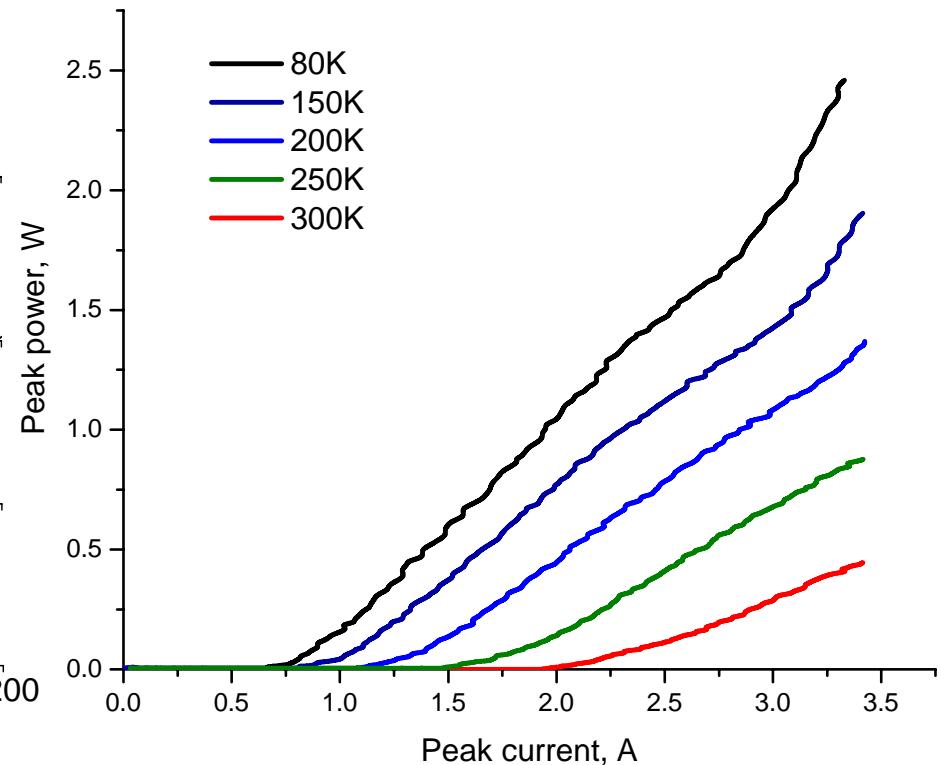
Device performance: mid-IR



Spectra



Power (combined)

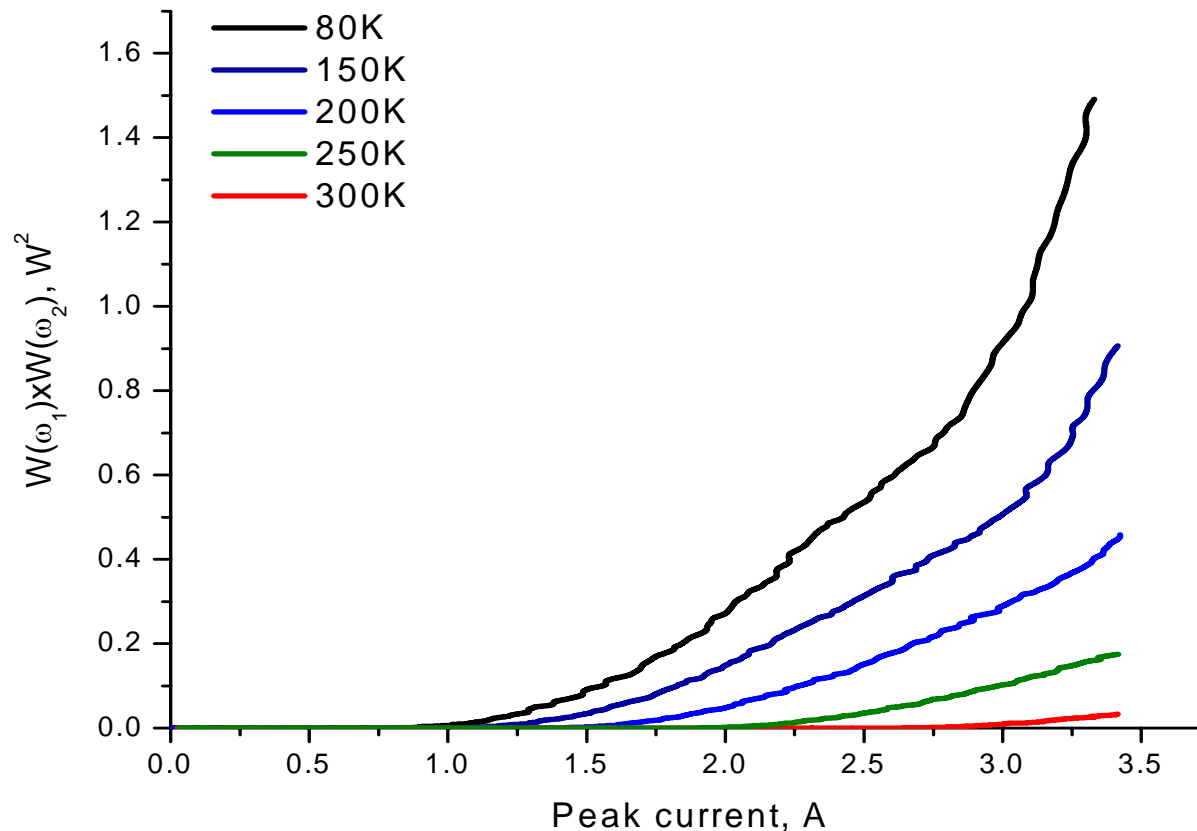


25- μm -wide, tapered to 50- μm -wide, 2-mm-long, back facet HR coating.
Testing in pulsed mode (60ns pulses at 250kHz).

Product of the pump powers

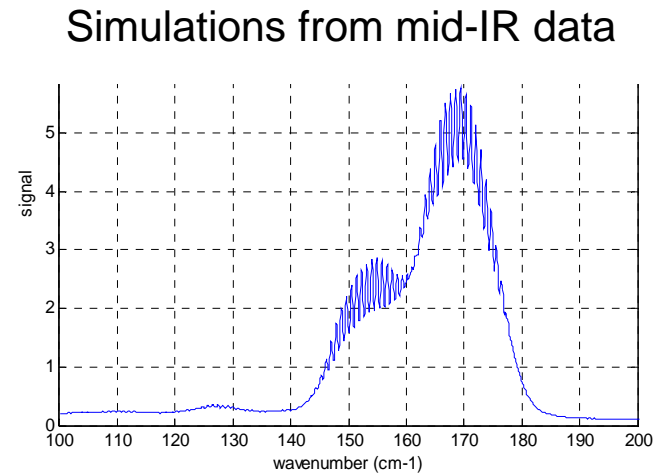
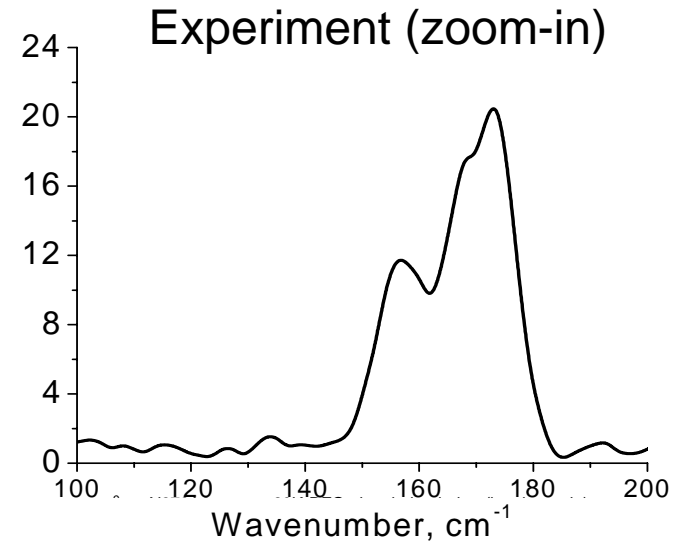
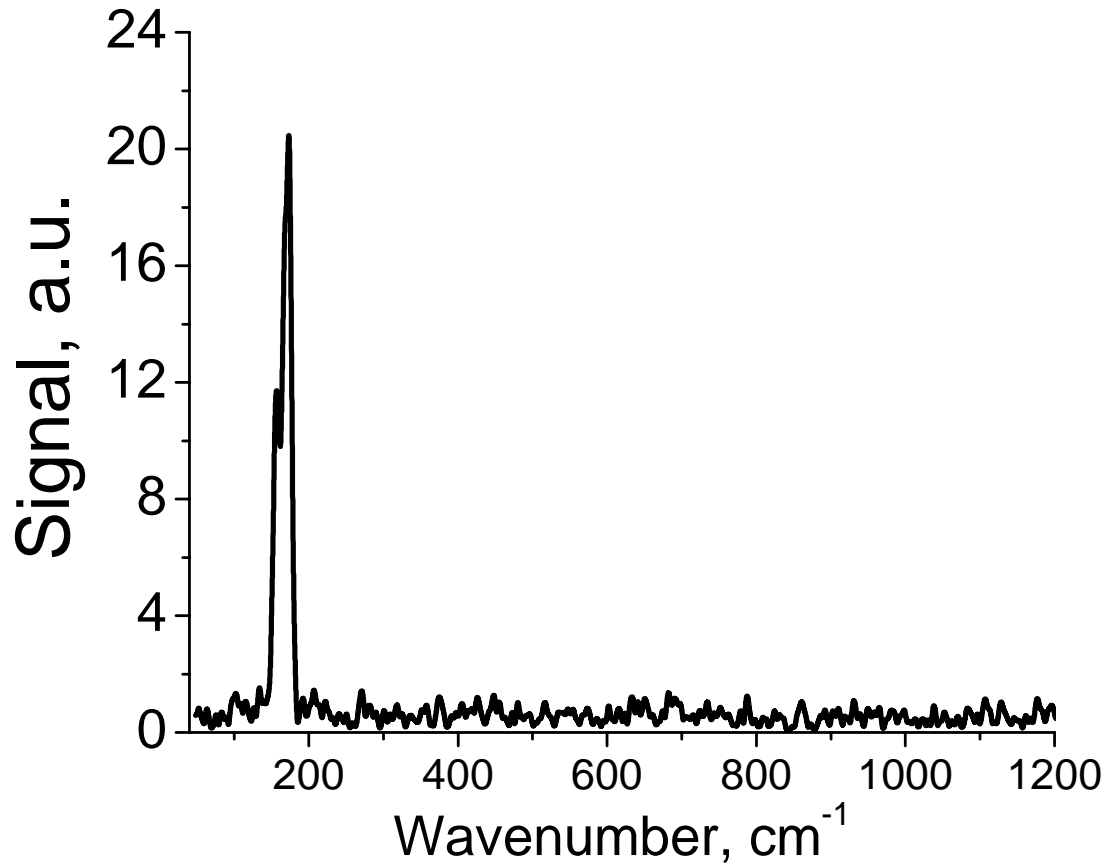


$$W(\omega_{THz}) \propto |\chi^{(2)}|^2 W(\omega_1)W(\omega_2) \times l_{eff}^2$$



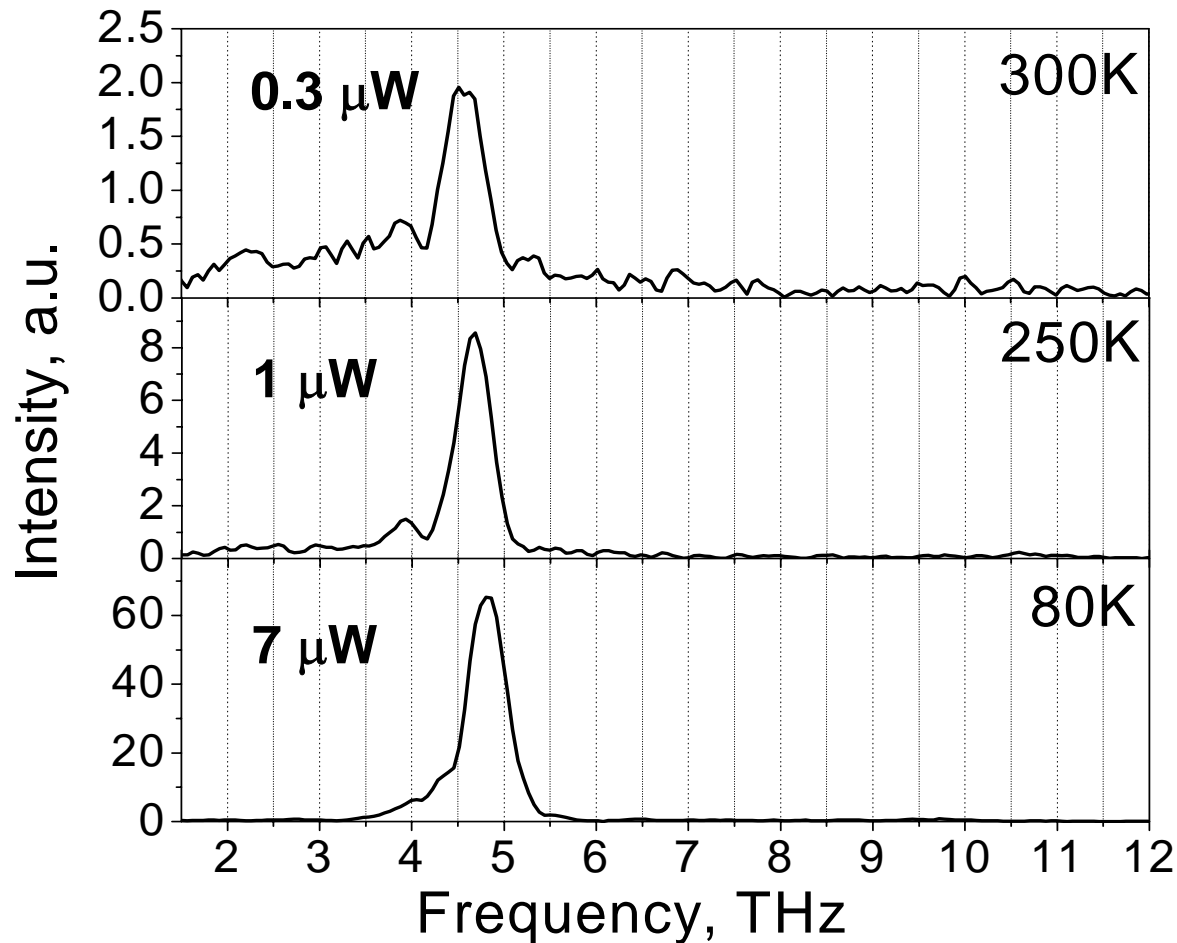
25- μ m-wide, tapered to 50- μ m-wide, 2-mm-long, back facet HR coating.
Testing in pulsed mode (60ns pulses at 250kHz).

Terahertz emission 80K



25- μm -wide, tapered to 50- μm -wide, 2-mm-long, back facet HR coating.
Testing in pulsed mode (60ns pulses at 250kHz).

Terahertz output at different T



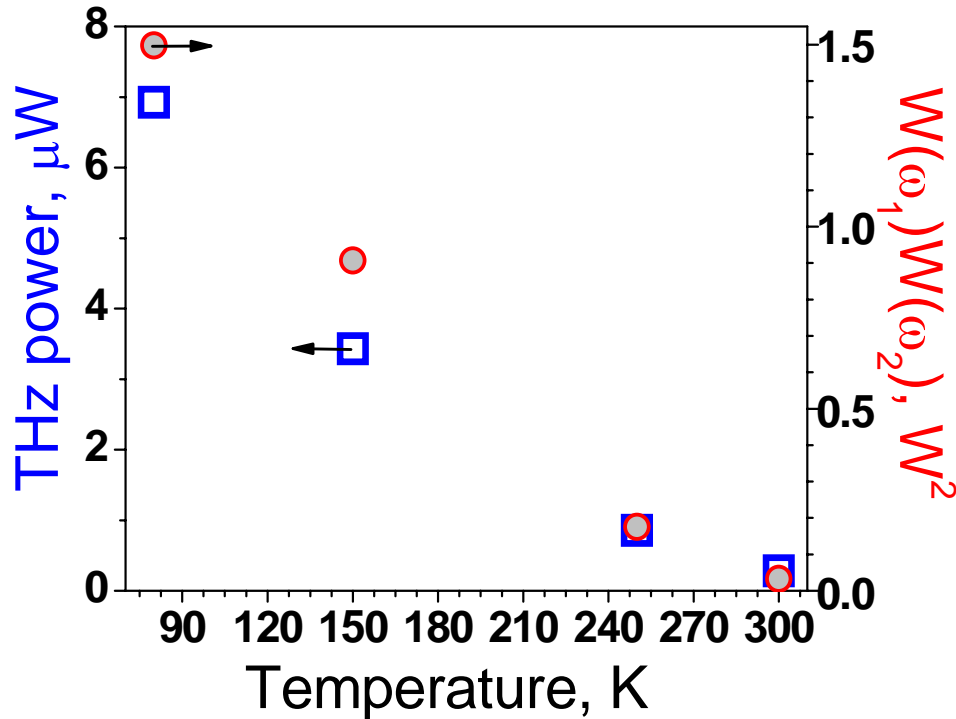
- Peak positions agree with mid-IR data
- Red-shift with temperature can also be observed in mid-IR data
- THz DFG signal observed up to room temperature

25-μm-wide, tapered to 50-μm-wide, 2-mm-long, back facet HR coating, + Silicon lens
Testing in pulsed mode (60ns pulses at 250kHz).

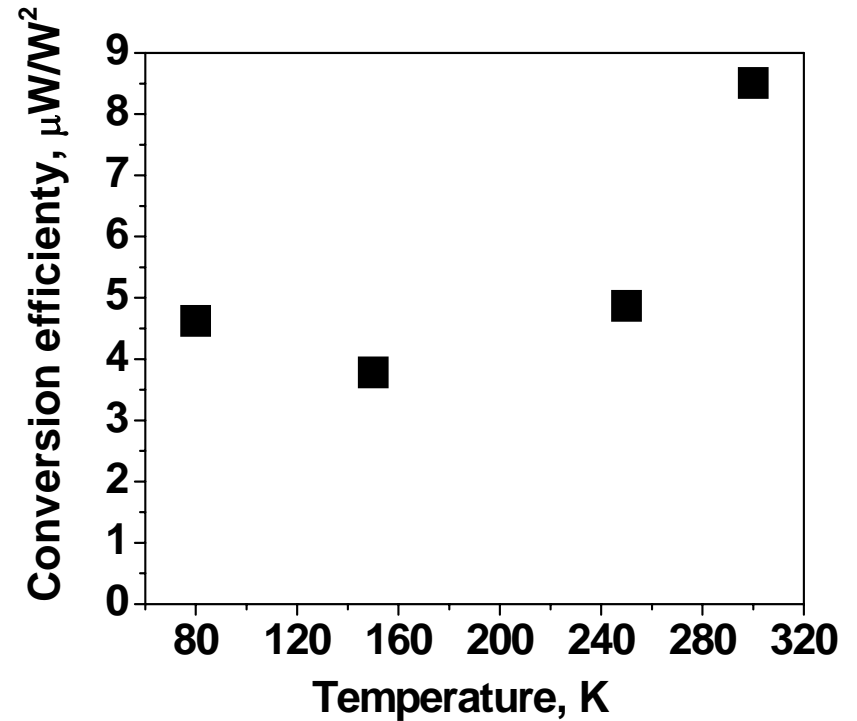
Conversion efficiency at different T



Peak THz and mid-IR power vs T



Conversion efficiency vs T



Conversion efficiency $\sim 5 \mu\text{W}/\text{W}^2$

Conversion efficiency: analysis



$$W_{\text{THz}} \approx \frac{\omega^2}{8\epsilon_0 c^3 n_{\text{eff}}^\omega n_{\text{eff}}^{\omega_1} n_{\text{eff}}^{\omega_2}} \times \frac{|\chi^{(2)}|^2}{S_{\text{eff}}} W_1 W_2 \times l_{\text{eff}}^2$$

S_{eff} , l_{eff} , refractive indices are known from waveguide calculations:

$$n_{\text{eff}} \approx 3, l_{\text{eff}} \approx 70 \mu\text{m}, S_{\text{eff}} \approx 1800 \mu\text{m}^2$$

Estimate $\chi^{(2)}$ using electron density in upper laser state from gain=loss condition:

$$\chi^{(2)} \approx 3 \times 10^4 \text{ pm/V}$$

Uncertain parameters:

Mid-IR lasing in higher order lateral modes

THz wave out-coupling efficiency from QCL waveguide (~30%?)

Conversion efficiency: analysis



$$W_{\text{THz}} \approx \frac{\omega^2}{8\epsilon_0 c^3 n_{\text{eff}}^\omega n_{\text{eff}}^{\omega_1} n_{\text{eff}}^{\omega_2}} \times \frac{|\chi^{(2)}|^2}{S_{\text{eff}}} W_1 W_2 \times l_{\text{eff}}^2$$

S_{eff} , l_{eff} , refractive indices are known from waveguide calculations:

$$n_{\text{eff}} \approx 3, l_{\text{eff}} \approx 70 \mu\text{m}, S_{\text{eff}} \approx 1800 \mu\text{m}^2$$

Estimate $\chi^{(2)}$ using electron density in upper laser state from gain=loss condition:

$$\chi^{(2)} \approx 3 \times 10^4 \text{ pm/V}$$

Uncertain parameters:

Mid-IR lasing in higher order lateral modes

THz wave out-coupling efficiency from QCL waveguide (~30%?)

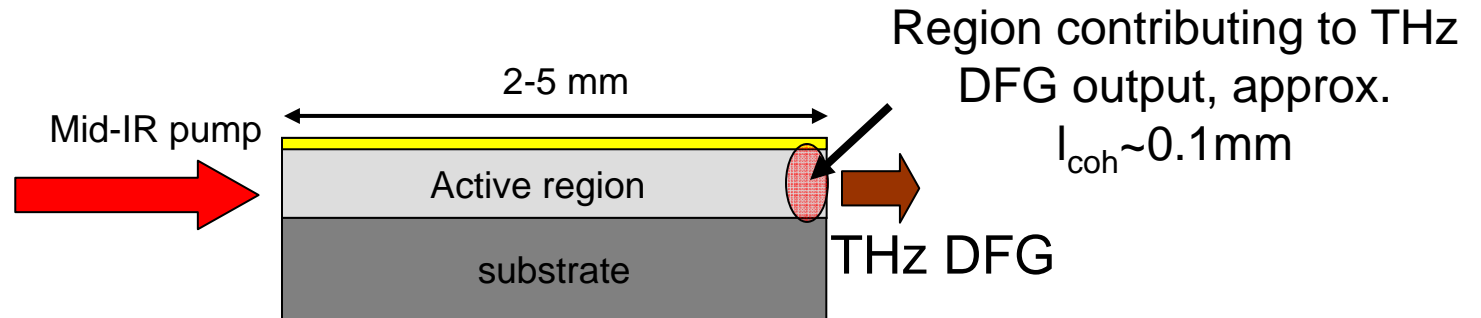
Theoretical efficiency: $W_{\text{THz}} / (W_1 \times W_2) \sim 30 \mu\text{W/W}^2$

Experiment (corrected for the collection efficiency): $\sim 5 \mu\text{W/W}^2$

Need for surface extraction of DFG

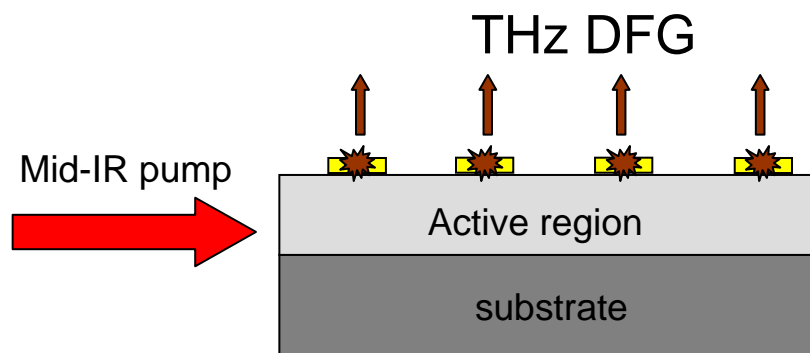


Edge emitting THz DFG is not efficient



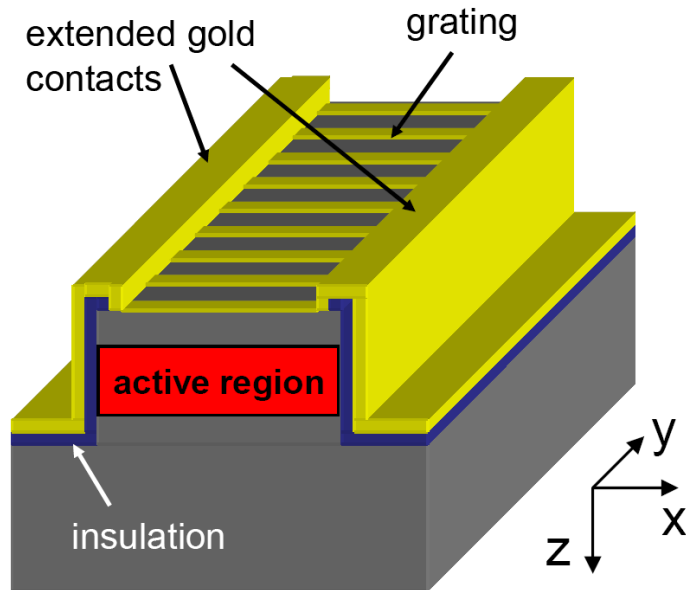
Only a small section $\sim l_{coh}$ contributes to THz DFG output

Surface-emitting scheme to boost THz power



The whole device contributes to THz DFG

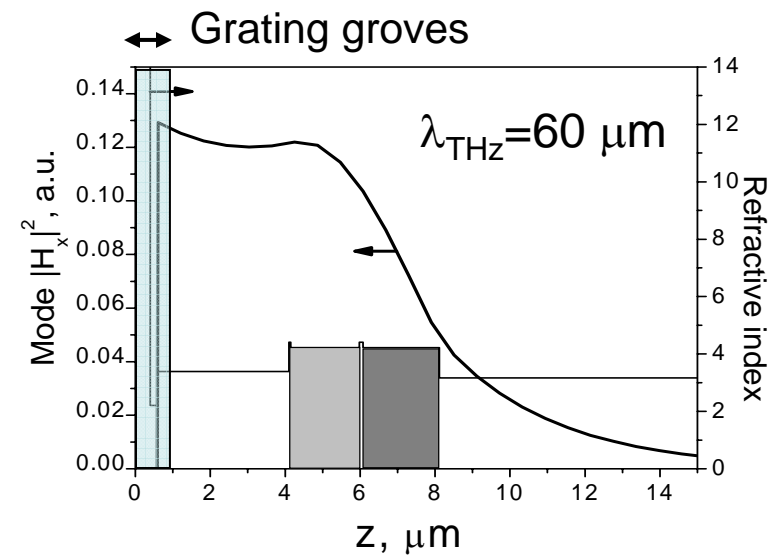
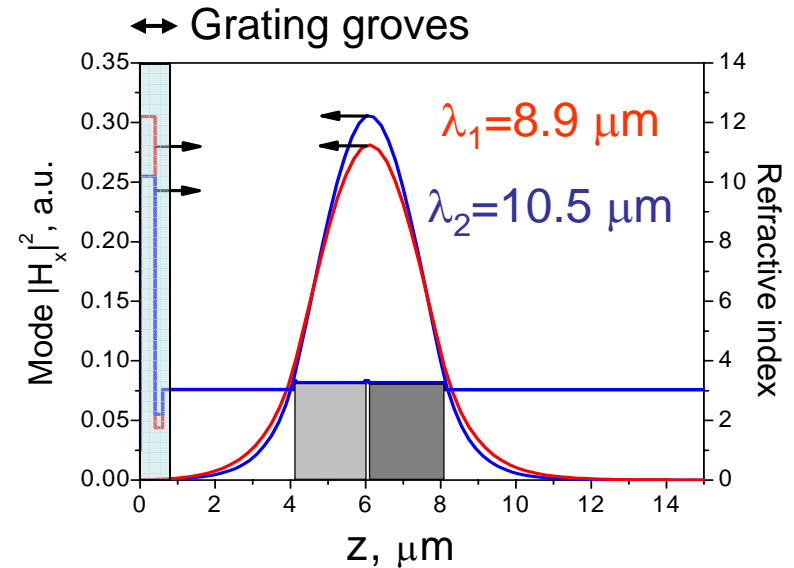
Device design for surface emission



THz radiation is produced by $P^{(2)}$

$$P^{(2)}(\omega_{\text{THZ}}=\omega_1-\omega_2)\sim\chi^{(2)}E(\omega_1)E(\omega_2)e^{i(k_1-k_2)y}$$

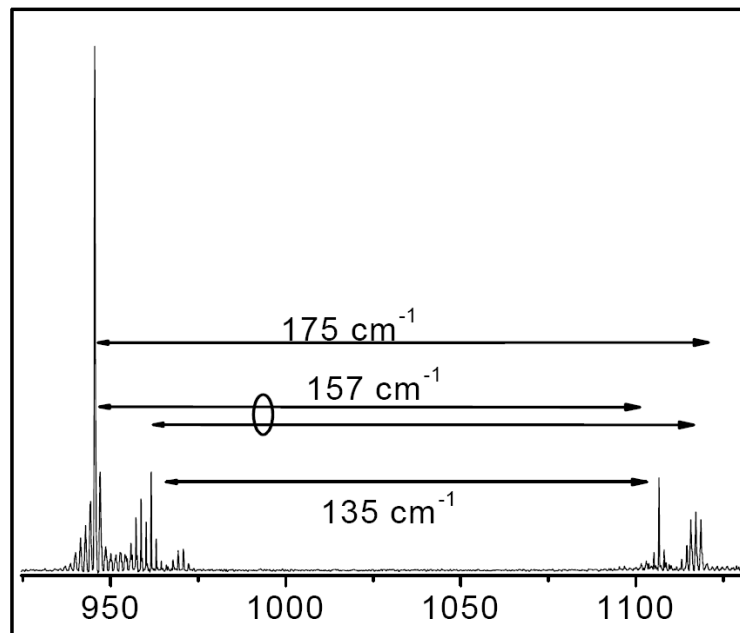
For efficient vertical outcoupling, we need the grating k-vector $k_{\text{gr}}=k_1-k_2$



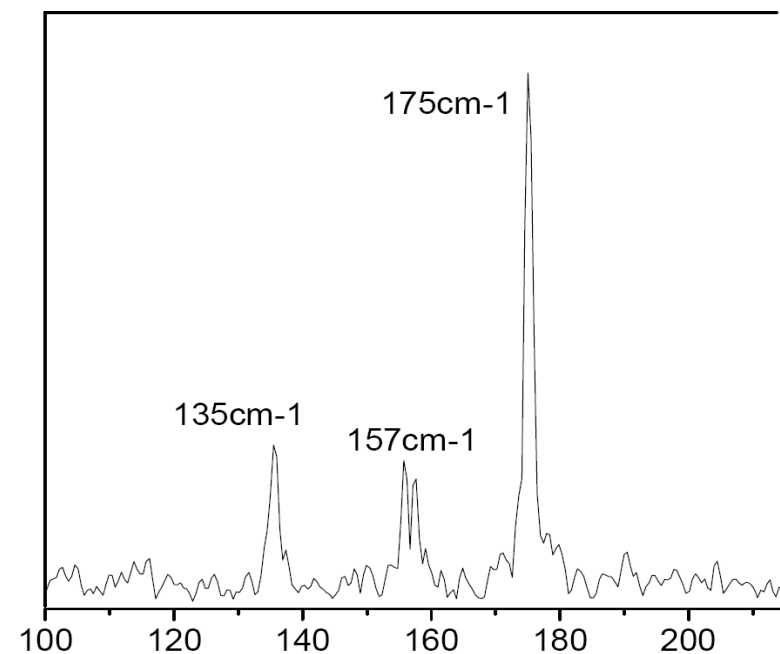
Surface emission



Edge-emission mid-IR spectrum



Surface-emission THz spectrum

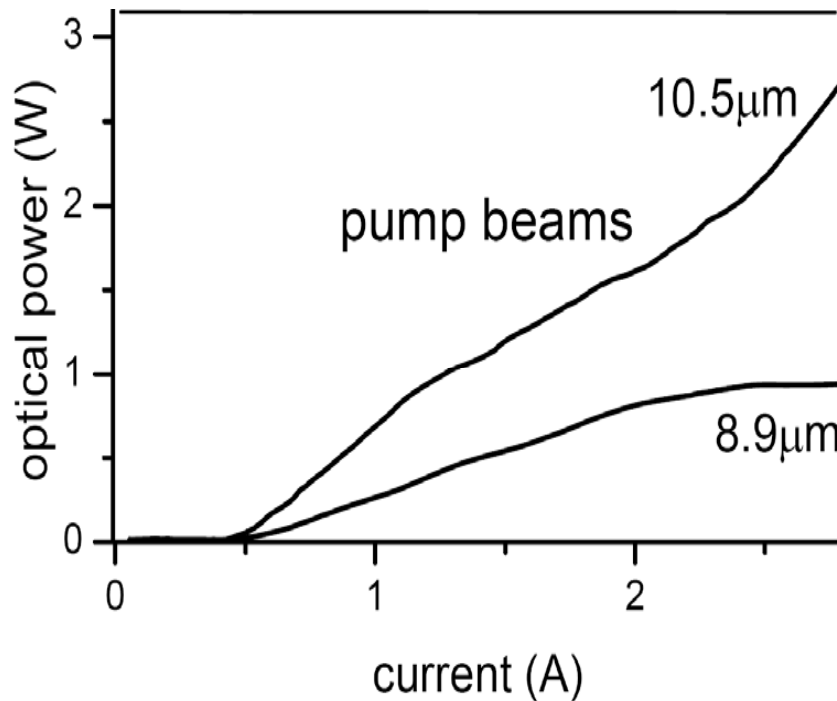


25- μm -wide, with second order grating for THz DFG, 1-mm-long, back facet HR coating. Testing in pulsed mode (60ns pulses at 250kHz) with 3.5A current pulses at 80K.

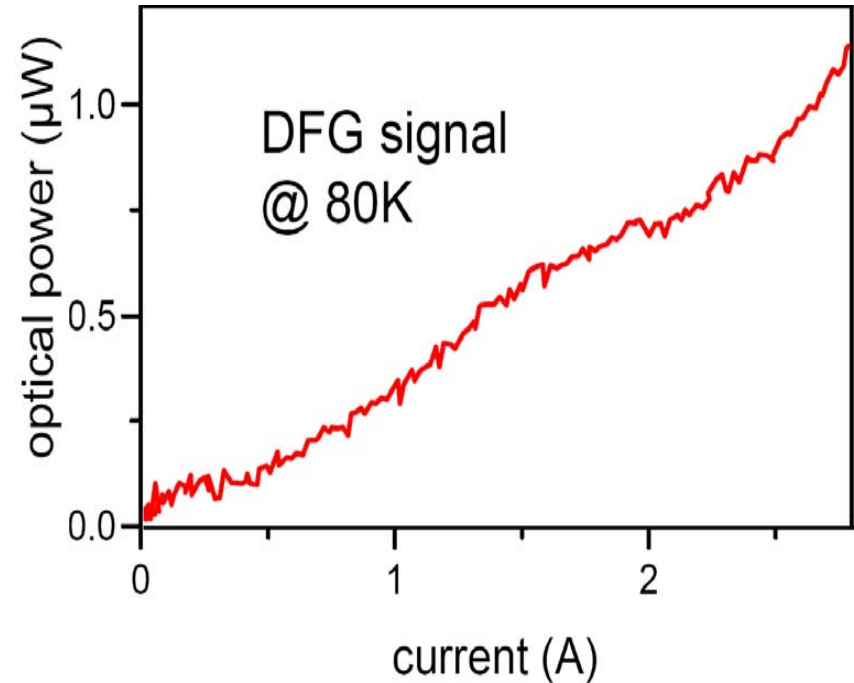
Power output



Edge emission mid-IR power



Surface emission THz power

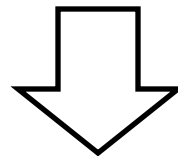


25-μm-wide, with second order grating for THz DFG, 1-mm-long, back facet HR coating. Testing in pulsed mode (60ns pulses at 250kHz) with 3.5A current pulses at 80K.

Future improvements



- *Improve waveguide designs for larger I_{coh}*
- *Improve active region designs for higher $\chi^{(2)}$*
- *Improved surface emission for more outcoupling*
- *Mode-locking for higher peak intensity*



mW-level THz DFG QCL sources

Acknowledgements



People

Harvard: *Federico Capasso, Christian Pflügl, Jonathan Fan, Qijie Wang, Laurent Diehl, Sahand Hormoz.*

Texas A&M: *Alexey Belyanin, Feng Xie*

University of Leeds: *Edmund Linfield, Suraj Khanna, Mohamed Lachab, Giles Davies*

University of Paris: *Raffaele Colombelli, Yannick Chassagneux*

ETH-Zürich: *Jérôme Faist, Milan Fischer, Andreas Wittmann*

Funding

AFOSR FA9550-05-1-0435

Postdoc opportunities



University of Texas, Austin



City of Austin



mbeikin@ece.utexas.edu
<http://www.ece.utexas.edu/~mbeikin/>